References

1 LO, T.K.: 'Miniature aperture-coupled microstrip antenna of very high permittivity', *Electron. Lett.*, 1997, **33**, pp. 9–10

2 PINHAS, S., and SHTRIKMAN, S.: 'Comparison between computed and measured bandwidth of quarter-wave microstrip radiators', *IEEE Trans.*, 1988, **AP-36**, (11), pp. 1615–1616

3 WATERHOUSE, R.B.: 'Small microstrip patch antenna', *Electron. Lett.*, 1995, **31**, pp. 604–605

4 LUK, K.M., CHAIR, R., and LEE, K.F.: 'Small rectangular patch antenna, *Electron. Lett.*, 1998, **34**, pp. 2366–2367

Spatial aliasing for near-field sensor arrays

T.D. Abhayapala, R.A. Kennedy and R.C. Williamson

An investigation is presented into the presence of spatial aliasing due to the operation of a linear array in the near-field. It shows that the standard half wavelength sensor spacings rule, which guarantees that no aliasing will occur in the operation of far-field arrays, is not sufficient to prevent aliasing in the near-field. This claim is justified by theoretical considerations and corroborated by simulation results.

Introduction: There has been a growing interest in near-field array processing due to the use of microphone arrays in teleconferencing and speech acquisition systems [1 – 3]. In this Letter we consider the effect of spatially sampling a spherical wavefront received from a point source in the near-field of a linear array, along the array axis.

Spatial aliasing: Consider a linear array aligned to the x axis and a point source at a distance r from the array origin and angle θ measured relative to endfire. The signal received at a point x on the array is given by

$$s_{r,\theta}(x) = \frac{e^{jk\sqrt{r^2+x^2-2rx\cos\theta}}}{\sqrt{r^2+x^2-2rx\cos\theta}} \qquad (1)$$

where $k = 2\pi/\lambda$ is the wavenumber and λ is the wavelength of the received signal. If the source of interest is in the far-field of the array, then the normalised signal received at a point x on the array is given by

$$s_{\infty,\theta}(x) = \lim_{r\to\infty} s_{r,\theta}(x) r e^{-jkr} = e^{-jkx\cos\theta} \qquad (2)$$

By using an array, we effectively sample the signal $s_{r,\theta}(x)$ in the spatial domain. To determine the sampling distance, i.e. array spacings, we need to examine the spectral content of the signal $s_{r,\theta}(x)$ with respect to x. Let the Fourier transform of $s(x)$ be

$$S(\xi) = \int_{-\infty}^{\infty} s(x) e^{j\xi x} dx \qquad (3)$$

where ξ is the spatial frequency. Using eqn. 3, we can write the Fourier transform of eqn. 2 as

$$S_{\infty,\theta}(\xi) = 2\pi\delta(\xi - k\cos\theta) \qquad (4)$$

where $\delta(\cdot)$ is the Dirac delta function. Considering the usual Nyquist criterion, we need to sample $s_{\infty,\theta}(x)$ with a sampling distance of $d \le \pi/(k\cos\theta)) = \lambda/(2\cos\theta)$ to avoid spatial aliasing. Since we assume that the possible range of $\theta \in [0, \pi]$, it suffices to take $d_{max} = \lambda/2$. This result, commonly known as the $\lambda/2$ rule, is standard in the array literature [4]. To date, this rule has been used for designs in both the far-field and near-field (e.g. [5]). We show here that the $\lambda/2$ rule is generally not valid in the near-field.

The Fourier transform $S_{r,\theta}(\xi)$ of $s_{r,\theta}(x)$ can be obtained from the results in [6]

$$S_{r,\theta}(\xi) = \begin{cases} j\pi e^{jr\xi\cos\theta} H_0^{(1)}\left(r\sin\theta\sqrt{k^2-\xi^2}\right) & |\xi| < k \\ 2e^{jr\xi\cos\theta} K_0\left(r\sin\theta\sqrt{\xi^2-k^2}\right) & |\xi| > k \end{cases}$$

where $H_0^{(1)}(\cdot)$ is the Hankel function ofthe first kind of order zero and $K_0(\cdot)$ is the modified Bessel function of order zero. Note that there is a singularity at $|\xi| = k$.

A graph of $|S_{r,\theta}(\xi)|$ against normalised spatial frequency ξ/k for three different sets of values (r,θ) is shown in Fig. 1. From this result, it is evident that the function $s_{r,\theta}(x)$ is not bandlimited if the source is in the near-field of the array at a smaller angle measured relative to the endfire, although it becomes more so as $r \to \infty$ or $\theta \to 90°$. Thus, the use of the $\lambda/2$ rule is not strictly sufficient to ensure no aliasing error, and indeed no sampling distance will entirely eliminate such an error.

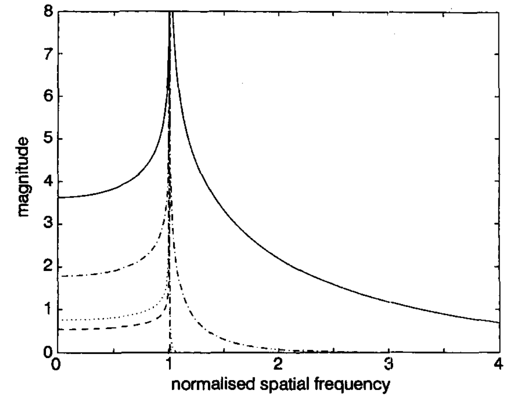

Fig. 1 *Magnitude of Fourier transform $S_{r,\theta}(\xi)$ of the signal $s_{r,\theta}(x)$ against normalised spatial frequency ξ/k*

——— $r = 3.5\lambda$, $\theta = 1°$
– · – · $r = 3.5\lambda$, $\theta = 5°$
– – – – $r = 3.5\lambda$, $\theta = 90°$
·········· $r = 100\lambda$, $\theta = 1°$

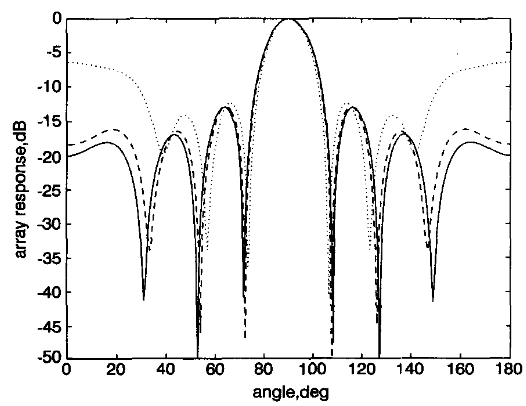

Fig. 2 *Magnitude of array response to near-field source at 3.5λ from array origin*

·········· $\lambda/2$ spaced 7 sensor array
– – – – $\lambda/4$ spaced 13 sensor array
——— $\lambda/6$ spaced 37 sensor array
Aperture length of each of three arrays equal to 3λ

Near-field rule of thumb: To explain the above behaviour, we now examine $S_{r,\theta}(\xi)$ when $\xi > k$ for different values of r and θ. Since $K_0(z) \simeq -\ln(z)$ for $z \to 0$ and $K_0(z) \simeq \sqrt{[\pi/(2z)]}e^{-z}$ for large $z > 1$ [7], $|S_{r,\theta}(x)|$ decays rapidly as the argument of $K_0(\cdot)$ (i.e. $r\sin\sqrt{[\xi^2-k^2]}$) increases. Suppose there exists positive numbers M and z_0 such that $|S_{r,\theta}(\xi)| < M$ for $r\sin\sqrt{(\xi^2-k^2)} > z_0$ for a given r and θ. Then for a suitably small M we can assert that $S_{r,\theta}(\xi)$ is approximately bandlimited by

$$\xi_0 = \sqrt{k^2 + \frac{z_0^2}{r^2\sin^2\theta}} \qquad (5)$$

and a sampling distance of π/ξ_0 or less reduces the aliasing up to an acceptable level. It is difficult to find an analytic expression for z_0 in terms of M or quantify an acceptable level of aliasing. However, a convenient rule of thumb is $z_0 \simeq 1$.

Note that when $r \to \infty$, $\xi_0 \to k$, hence $S_{r,\theta}(\xi)$ is bandlimited by k for this case. For $\theta = 90°$, $\xi_0 = \sqrt{[k^2 + 1/r^2]} \simeq k$ for all practical values of r in the near-field. For example if $r = 3\lambda = 6\pi/k$ then $\xi_0 = k\sqrt{[1 + 1/36\pi^2]} \simeq k$. Hence, for angles close to 90°, $S_{r,\theta}(\xi)$ is bandlimited by k even for near-field signals. However, near-field signals from small angles are not spatially bandlimited which can be deduced from eqn. 5.

Simulations and conclusion: To conclude we show the effect of spatial aliasing due to sampling a signal from a near-field source at 3.5λ from an array origin, where λ is the wavelength of the signal. Fig. 2 shows the magnitude response of three arrays with different sensor spacings of $\lambda/2$, $\lambda/4$ and $\lambda/6$, to the above source as a function of θ. For comparison, we make all three arrays have equal aperture length, thus they have 7, 13 and 19 elements, respectively. The effect of aliasing is clearly evident from the response of the $\lambda/2$ spaced array, however there is little or no effect of aliasing present in the response of the $\lambda/6$ spaced array. This result is in agreement with eqn. 5 which gives a sensor spacing of $\lambda/5.6$ to avoid aliasing for $r = 3.5\lambda$ and $\theta = 1°$.

Thus we can conclude that the received signal from a point source in the near-field is not bandlimited in spatial frequency and hence the use of standard half wavelengths spaced arrays introduces undesirable aliasing effects to the array output. The use of finer sensor spacings can overcome limitations imposed by aliasing.

Acknowledgment: This work was partially supported by the Australian Research Council.

11 March 1999
Electronics Letters Online No: 19990561
DOI: 10.1049/el:19990561

T.D. Abhayapala and R.A. Kennedy (*Telecommunications Engineering Group, Research School of Information Sciences and Engineering, Australian National University, Canberra ACT 0200, Australia*)

R.C. Williamson (*Department of Engineering, Faculty of Engineering and Information Technology, Australian National University, Canberra ACT 0200, Australia*)

References

1 FLANAGAN, J.L., BERKELEY, D.A., ELKO, G.W., WEST, J.E., and SONDHI, M.M.: 'Autodirective microphone systems', *Acoustica*, 1991, **73**, pp. 58–71

2 KHALIL, F., JULLIEN, J.P., and GILLOIRE, A.: 'Microphone array for sound pickup in teleconference systems', *J. Audio Eng. Soc.*, 1994, **42**, pp. 691–700

3 NORDHOLM, S., REHBOCK, V., TEO, K.L., and NORDEBO, S.: 'Chebyshev optimization for the design of broadband beamformers in the near field', *IEEE Trans.*, 1998, **CASII-45**, pp. 141–143

4 FLANAGAN, J.L.: 'Beamwidth and useable bandwidth of delay-steered microphone arrays', *AT&T Tech. J.*, 1985, **64**, pp. 983–995

5 GRENIER, Y.: 'A microphone array for car environments', *Speech Commun.*, 1993, **12**, pp. 25–39

6 ERDELYI, A. (Ed.): 'Tables of integral transforms, Vol II (McGraw-Hill, New York, 1954)

7 McLACHLAN, N.W.: 'Bessel functions for engineers' (Oxford University Press, London, 1961)

Noninvasive estimation of left-ventricular end-diastole elasticity by analysing heart wall vibrations

H. Kanai, S. Nakaya, H. Honda and Y. Koiwa

A new noninvasive method was previously presented for the measurement of the left ventricular (LV) end-diastolic pressure (EDP) by combining Mirsky's method and the experimentally derived relationship. The eigenfrequency was determined by applying a short-time Fourier transform to the velocity signal on the human heart wall which is transcutaneously measured *in vivo* by the phased tracking method using ultrasound. In the Letter the authors estimate the elasticity of the heart wall for several human patients.

Introduction: Left ventricular (LV) pressure and its elasticity are significant parameters necessary for the clinical diagnosis of heart diseases. In particular, knowledge of the LV end-diastolic pressure (EDP), P_{ED}, is usually needed to assess LV functioning in clinical settings; a noninvasive method to measure this was previously presented [1]. The eigenfrequency was found by using a short-time Fourier transform to the velocity signal on the human heart wall [2] which is measured transcutaneously *in vivo* by the phased tracking method [3] using ultrasound. However, the LV EDP, the normal value of which lies between 5 and 12mmHg, cannot be obtained from the blood pressure measured at the brachial artery. Furthermore, the LV end-diastolic elasticity (EDE) E_{ED} cannot be noninvasively measured. To measure the LV pressure of a patient, invasive catheterisation is essential. Although the accuracy of this measurement has been confirmed, such cardiac catheterisation is difficult to apply at the bedside. Therefore, a noninvasive technique for measuring of LV EDP, P_{ED}, and its elasticity, E_{ED}, is needed.

Based on dimension analysis and Advauni and Lee's equation [4], by assuming that the LV wall vibration at the end-diastole is approximated by the free vibration of an elastic shell, Honda *et al.* [5] have experimentally derived a simple relationship between Young's modulus E [Pa] of the LV wall, the LV internal radius r [m], the LV wall thickness h [m], the myocardial density ρ [kg/m³], and the LV instantaneous mode-2 eigenfrequency f_2 [Hz] as follows:

$$r \cdot f_2 = A\left(\frac{h}{r}\right)\sqrt{\frac{E}{\rho}} \quad [\mathrm{m/s}] \tag{1}$$

where the coefficient $A(h/r)$ is a function of h/r and is independent of elasticity. From Honda's experiment [4], the values of $A(h/r)$ are determined for various values of h/r and it is experimentally found out that $A(h/r)$ does not strongly depend on the values of h/r. By assuming a myocardial density ρ of 1.02×10^3 [kg/m³], eqn. 1 is approximated by

$$E = 1.02 \times 10^3 \frac{1}{A\left(\frac{h}{r}\right)} r^2 f_2^2 \quad [\mathrm{Pa}] \tag{2}$$

It is worth noting that the elasticity E of the shell is noninvasively estimated without measuring the LV EDP when r, h, and f_2 are measured.

In Mirsky's method [6], on the other hand, the LV elastic stiffness E_q [Pa] is given by

$$E_q = 399\left(1+\frac{V_w}{V}\frac{r^2}{r^2+(r+h)^2}\right)\left(1+\alpha V+\frac{\beta V}{P_{ED}}\right)\sigma_m \quad [\mathrm{Pa}] \tag{3}$$

where $V = 4\pi r^3/3$ [m³] and $V_w = 4\pi((r + h)^3 - r^3)/3$ [m³] are the internal and wall volumes, respectively, $\sigma_m = V/V_w \times (1 + (r + h)^3/2R^3)P_{ED}$ [Pa] is the stress on the LV wall, and $R = r + h/2$. The coefficients α and β satisfy the relationship $dP_{ED}/dV = \alpha \cdot P_{ED} + \beta$. It is experimentally found that β is negligibly small and α is given by $P_{ED} = 57.32e^{\alpha V}$.

By assuming that the E of eqn. 2 is equal to the E_q of eqn. 3, the LV EDP P_{ED} is determined from the eigenfrequency f_2 of the LV wall vibration, where the internal radius r, and the thickness h, are easily measured by echocardiography. The LV wall vibration $y(t)$ is transcutaneously measured by the novel phased tracking method [3] developed in our laboratory using ultrasound. By applying a short-time Fourier transform to the resultant $y(t)$, its eigenfrequency f_2 is determined at the end-diastole. At the same time, the LV EDE E_{ED} is obtained from eqn. 2.

In vivo experimental results: Fig. 1*a* and *b* show a typical example of the electrocardiogram (ECG) and the vibration $y(t)$, respectively, on the LV side of the interventricular septum (IVS) measured by the phased tracking method of a 60 year old male patient (A) with mitral regurgitation (MR). By referring to the cross-sectional B-mode image, the direction of the ultrasonic beam is set so that the beam is perpendicular to the IVS during the measurement. Fig. 1*c* shows the time-frequency distribution of $y(t)$ of Fig. 1*b*. The instantaneous eigenfrequency f_2 of mode 2 is determined for the five instants at the end-diastole. With the determined f_2, the LV EDP P_{ED} is calculated for each instant t as shown by the squares in Fig. 1*d* using eqns. 2 and 3. The resultant pressure